

# Morphology of retinal vessels in the optic disk in a Göttingen minipig experimental glaucoma model

Marta Galdos,<sup>\*,†</sup> Alejandro Bayón,<sup>‡</sup> Francisco D. Rodríguez,<sup>§</sup> Carlos Micó,<sup>¶</sup> Sansar C. Sharma<sup>\*\*</sup> and Elena Vecino<sup>††</sup>

<sup>\*</sup>Department of Ophthalmology, Hospital de Cruces, University of the Basque Country (UPV/EHU), Vizcaya, Spain; <sup>†</sup>Department of Cell Biology and Histology, University of the Basque Country (UPV/EHU), Vizcaya, Spain; <sup>‡</sup>Department of Veterinary Ophthalmology, Murcia University, Murcia, Spain; <sup>§</sup>Department of Biochemistry and Molecular Biology, University of Salamanca, Salamanca, Spain; <sup>¶</sup>Department of Veterinary Ophthalmology, Murcia University, Murcia, Spain; <sup>\*\*</sup>Department of Ophthalmology and Cell Biology, New York Medical College, Valhalla, NY, USA; and <sup>††</sup>Department of Cell Biology and Histology, University of the Basque Country (UPV/EHU), Vizcaya, Spain

Address communications to:

E. Vecino

Tel: +34-94-601-2820

Fax: +34-94-601-3266

e-mail: elena.vecino@ehu.es

## Abstract

**Objective** To compare the morphology of normal, healthy Göttingen minipig retinal vessels of the optic disk with experimentally induced glaucomatous optic disks in order to identify the glaucomatous excavation. Present results were compared to human glaucoma findings.

**Procedure** Sixteen eyes from eight Göttingen minipigs were studied using fundoscopic photography and fluorescein angiography. Experimental glaucoma was then induced in the left eyes over 14 months, and changes in the optic disk vessels were assessed using fundoscopic photography and fluorescein angiography. The changes were compared with those previously reported in humans.

**Results** Regarding the number of vessels, the location from where they emerge and the sectors of the optic disk that they cross, arterial and retinal vessels in Göttingen minipigs present a more asymmetric layout than in humans. The central excavation is filled by the central venous ring. Changes in the glaucomatous optic disk include arteriolar incurvation, and sometimes, nasal, and peripheral displacement of the arterioles that emerge between the ganglion cell axons of the neuroretinal ring. No angiographic changes were observed in the experimental glaucoma model.

**Conclusions** The changes in the glaucomatous optic disk of the minipig imply a predominant involvement of the arterioles. However, in humans with primary open-angle glaucoma (POAG), both the arterioles and the venules are displaced, and the central excavation is easier to distinguish, because of the absence of a central venous ring.

**Key Words:** arterioles, fluorescein angiography, glaucoma, minipig, optic disk, venules

## INTRODUCTION

The experimental glaucoma model in the Göttingen minipig<sup>1</sup> has proven to be very useful for research on the pathogenesis of glaucoma. The porcine (*Sus scrofa domestica*) eye has previously been validated as an experimental glaucoma model<sup>2,3</sup> and studies have been carried out on this model, regarding glaucoma physiopathogenesis<sup>4–6</sup> and neuroprotection.<sup>7,8</sup> However, the adult pig (*S. scrofa domestica*) presents a body weight that may reach up to 300 kg, making handling difficult in an experimental context. Göttingen laboratory minipigs are a reasonable alternative as they reach a final adult weight of between 35 and 55 kg.<sup>9</sup> The

angiographic and vascular corrosion casting studies conducted on the minipig retina show many similarities with reports on the human retina.<sup>10,11</sup>

The pig retina, like that of humans, is holangiotic,<sup>11</sup> i.e., retinal vessels are distributed in the internal two-thirds of the retina, while the external third, including photoreceptors, is nonvascular and is fed by the choroidal circulation. Also, both in pigs<sup>12</sup> and in humans,<sup>13</sup> retinal vessels have been considered as arterioles or venules as they present no internal elastic membrane (in the arterioles) and due to their small lumen diameter (in the venules). The trilaminar formation in porcine retinal capillaries is also similar to that of primates<sup>14</sup> because of their numerous intercon-

tions between the vascular layers. A general feature of species showing a holangiotic retina is the nonvascularization of some retinal regions, including areas next to the large vessels where oxygen diffusion could affect the retina.<sup>15</sup> In the pigs, there are also capillary-free areas around the principal arterioles, and similar areas can even be found surrounding the venules.<sup>11</sup> This finding has also been described in primates and in humans.<sup>14,16,17</sup> The presence of a nonvascular foveal region has been clearly demonstrated in primates and in humans.<sup>14,17–19</sup> In pigs, there is an area that only presents capillaries in the nerve fiber layer (macular area in humans). This area is characterized by a streaked pattern (Area centralis striaeformis) with a length of 25–30 mm and an absence of larger caliber retinal vessels. It spreads through the meridian from the temporal area to the nasal area and is only interrupted by the upper retinal arteriole and venule. There are numerous cones and a group of ganglion cells in this region that are denser than in any other retinal region.<sup>11</sup> The minipig eye has turned out to be especially adequate for experimental studies on retinal circulation because of its similarity with the human retina.<sup>10–12,20,21</sup> The porcine eye is different from other animals in that it has no reflective tapetum which is an important advantage for carrying out fluorescein angiographs. The porcine angiogram<sup>10</sup> is very similar to the pattern seen in primates.<sup>22,23</sup>

In humans, the changes in the optic disk are fundamental for glaucoma diagnosis. The lesion of the nerve fibers in glaucoma affects both the shape and area of the rim. A normal papilla shows a pattern that has a consistent rim width following the inferior, superior, nasal, and temporal (ISNT) rule: the inferior neuroretinal rim is generally wider than the superior one, followed by the nasal and finally, the temporal. This rule is very useful in clinical practice as any deviation increases suspicions of glaucoma damage.<sup>24</sup> Various patterns of glaucoma changes have been identified in humans.<sup>25,26</sup> Changes in rim width can be monitored, determining the cup/disk (C/D) ratio. Although this is easy to determine, it can also be misleading. Some small disks with a small C/D ratio can be pathological; however, larger, healthy disks can have a large C/D and look pathological.<sup>27</sup> Early changes in glaucoma optical neuropathy can be very subtle. These initial changes can be generalized, focal, and nonspecific. Some of the nonspecific changes include exposure of the lamina cribosa, nasal displacement of retinal vessels to the output of the optic disk, uncovering of circumferential vessels, and peripapillary atrophy.<sup>28</sup>

Taking into account the similarities between the minipigs retinal microvessels and those of the aforementioned angiographic pattern, and having an adequate experimental glaucoma model for this species, the morphology of retinal vessels in the control optic disk of the Göttingen minipig should be studied in detail. The aim of this article is to identify the disk excavation in the experimental glaucoma and to correlate it with human glaucoma.

## MATERIALS AND METHODS

### *Animals*

This study was carried out according to the Association for Research in Vision and Ophthalmology (ARVO) resolution on the use of animals in research. Eight Göttingen minipigs were used, four male and four female. The average age of the animals at the beginning of the experimental period was 5 months. The animals were kept under a 12:12 hour light/dark cycle and were fed once a day with water *ad libitum*.

### *Anesthesia and analgesic procedure*

The minipigs were anesthetized to conduct the angiography and the fundus eye test using the following drugs: 8 mg/kg tiletamine and zolazepam (Zoletil; Virbac, Esplugues de Llobregat, Spain), 0.04 mg/kg atropine, and 300 µg/kg medetomidine (Domitor; Esteve Veterinaria, Barcelona, Spain). The intraocular pressure (IOP) was measured after giving one drop of topical anesthesia (tetracaine + oxybutyprocaine drops). The surgical interventions were carried out under general anesthesia (10 mL/h propofol administered through an intravenous cannula inserted into the ear) as well as topical anesthesia (one drop of local anesthetic eye drops), with mechanical ventilation and monitoring of vital signs. After the operation and before the animal woke up, 1 g of intravenous Nolotil (metamizole) was injected as analgesic treatment.

### *Experimental glaucoma*

The surgical procedure was carried out following a technique previously reported for pigs<sup>2</sup> and minipigs.<sup>1</sup> Episcleral vein cauterization was performed on all left eyes (OSs), while ODs were left as the control group without intervention. Three episcleral veins of the OSs were cauterized at week 6. Three months after the first intervention (week 12), a second operation was carried out on the previously operated animals, with further cauterization of one ventral episcleral vein. Intraocular pressure was measured weekly using a Tono-Pen tonometer over 14 months. The statistical analysis used to compare IOP measurements in glaucomatous OSs and control ODs was the Wilcoxon signed-rank nonparametric test for related samples, SPSS 18.0 (software, SPSS PASW Statistics 18.0, SPSS Inc., Chicago, IL, USA).

### *Eye fundus photography*

All the animals were recorded using the same set-up: angiography equipment with a retinal camera (TRC-50XF; Topcon, Tokyo, Japan). Photographs of the posterior part of the eye and the optic disc of both REs and LEs in all eight animals were taken. The procedure was carried out in the operating theatre with the animal anaesthetized (protocol previously described). Fundus photographs were taken both at the beginning of the study (to obtain reference data for the 5-month-old minipigs) and at the end, after an average of 14 months of chronically increasing IOP.

### Fluorescein angiography procedure

Fluorescein angiography was performed on the OSs of eight animals using the same angiography equipment with a retina camera (Retinal camera TRC-50XF, Topcon) for all eight animals. Angiograms were performed after injection of a 0.2 mL/kg intravenous bolus of 10% fluorescein. Photographs were taken before fluorescein reached the choroidal vessels, in quick succession for the first 20 s, and then at slightly longer intervals to cover a total period of 3 min. The procedure was carried out in the operating theater with the animal anesthetized (protocol previously described). The initial angiographies enabled the collection of control data during normal phases in the minipig sample, while those taken at the end of the experimental period permitted the comparison of the eyes subjected to episcleral vein cauterization, with a subsequent increase in IOP, with the basal data from the controls.

### RESULTS

The fundoscopic description of the healthy ocular fundus of the Göttingen minipigs was carried out using the fundoscopic and angiographic photographs of both eyes taken in eight 5-month-old animals. Fluorescein angiography enables the differentiation of the retinal arterial circulation from the venous circulation by using contrasts in the arterioles in the retinal phase. The glaucomatous optic disk was assessed using fundoscopic and angiographic photographs of the OSs after 14 months of experimental glaucoma, and

comparing said photographs with the basal image taken at 5 months of age.

### Angiographic phases

Three angiographic phases were clearly distinguished: choroidal/arterial phase, arterial/venous phase and venous phase. Choroidal/arterial phase: The choroidal phase was found to overlap the arterial retinal phase in all animals. The choroidal contrast spread in a patchy pattern, showing areas of hyperfluorescence mixed with patches of hypofluorescence. The choroidal filling presented a typical granulated pattern. The choroidal filling in the animals, observable up to 7 s, lasted  $3.75 \pm 2.43$  s [mean value  $\pm$  Standard Deviation (SD)] and a median of 2 s. However, the delay in the peridiskal filling might appear in later times or even overlap with the arterial/venous phase and the venous phase (up to 25 s in one animal). Arterioles began to fill with contrast, marking the arterial phase, and the venules remained hypofluorescent without any contrast. The choroidal/arterial phase enabled the clear distinction of the arterial circulation from the venous circulation. In the choroidal/arterial phase, the optic disk became hyperfluorescent, especially in the inferior and nasal sections (Fig. 1). Arterial/venous phase was characterized by the presence of contrast in retinal venules. A laminar flow was typical, with fluorescence appearing only in the marginal area of the retinal venules, coming from dye from the capillary network. The arterial/venous phase in the animals subject to study lasted  $10.71 \pm 2.87$  s (mean value  $\pm$  SD), with a median of 12 s. The optic disk was com-

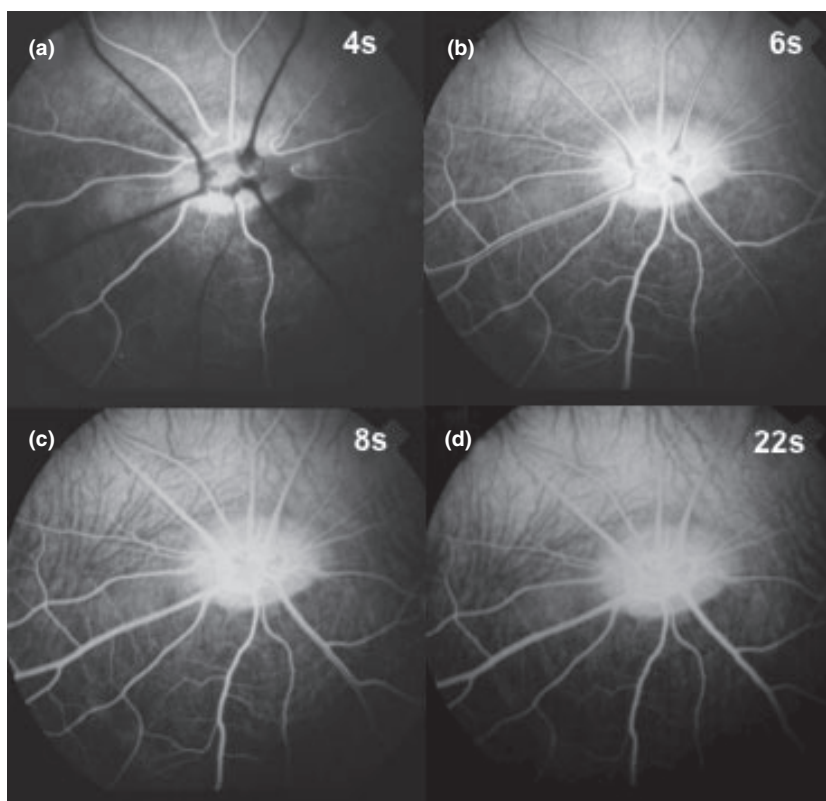


**Figure 1.** Angiographic phases in the Göttingen minipig. (a) Choroidal/arterial phase: the patched choroidal contrast filling is overlapped with the retinal arterioles that emerge in an independent manner and in a radial pattern. The optic disk begins to show hyperfluorescence in the inferior nasal sector. (b) Arterial/venous phase: peripheral laminar flow of the main venules forming the venous ring in the center of the optic disk is observed. The fluorescence of the optic disk is complete. (c–d) Venous phase: The main venules have completed the contrast filling in the axial area.

pletely fluorescent in this phase. In venous phase, the axial area of the venules was completely filled and retinal arterioles and venules were filled with contrast at the same time, so the capillary network was completely fluorescent. The venous phase was recorded in the animals over a mean value of time of 31.37 s (SD = 9.08) with a median of 30 s. The optic disk presented a greater fluorescence than in previous times, making it difficult to differentiate the vessels in the optic disk. After the first minutes, the choroidal fluorescence with a granulated pattern turned into a diffuse background fluorescence mixed with the hypofluorescence of the choroidal vessels without dye.

#### Morphology of the optic disk

The optic disk of the minipig presented a homogenous size in all the animals, with a vertical diameter of 1.5 mm and a horizontal diameter of 2.5 mm approximately. The large size of the optic disk, especially regarding its horizontal diameter, left a space large enough to hold the multivascular venous ring that spreads further into the horizontal diameter. This central venous ring fills the center of the optic disk corresponding with the lamina cribosa, making its visualization difficult. The neuroretinal ring was found in the periphery of the venous ring.

#### Retinal venous circulation in the minipig

The venous retinal circulation in the minipig was different from the arterial circulation, draining into the common venous ring found in the center of the optic disk cup. The venous ring, which presented different morphologies, covered the central area of the optic disk that corresponded with the lamina cribosa.

The total number of vessels of the venous system was  $7.31 \pm 1$  venules (mean value  $\pm$  SD). Venules of two different calibers converge in the central venous ring; on average, there were 3.69 (SD = 1) and 3.63 smaller (SD = 1) venules. The morphology of the venous ring was primarily determined by the large caliber venules. Main venules presented a greater caliber than retinal arterioles. We observed at least four different venous ring morphologies (Fig. 2): triangular (three main venules), rhomboidal (four main venules), quadrangular (four main venules), and hexagonal (6–7 main venules). The triangular pattern was the most frequent in the sample (62.6% of the eyes).

Considering the superior sector as having the 12 o'clock position, the temporal at 3 o'clock, the inferior at 6 o'clock, and the nasal at 9 o'clock, the rest of the sectors were designed as superotemporal, inferotemporal, inferonasal, and superonasal. Venules appeared more frequently in the

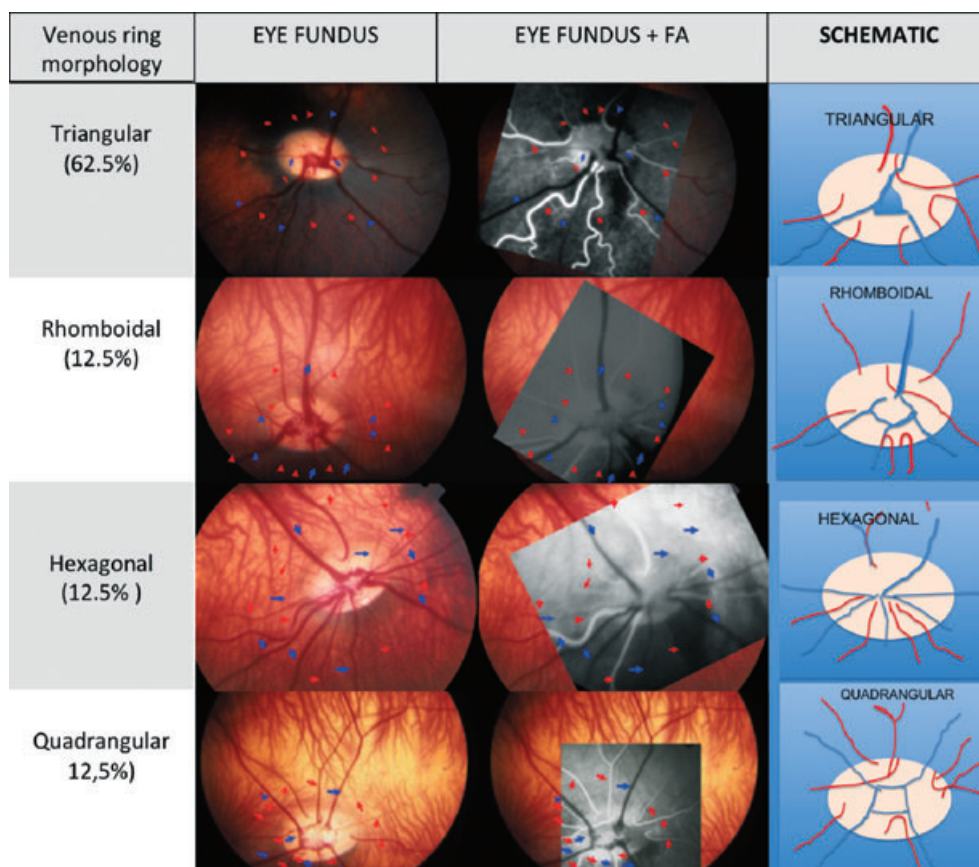


**Figure 2.** Morphology types of the central venous ring. Triangular (three main venules), rhomboidal (four main venules), quadrangular (four main venules), and hexagonal (6–7 main venules). The morphology of the triangular ring was the most frequent in the sample (62%). The arterial system is distinguished from the venous system using fluorescein angiography (FA) in the choroidal/arterial phase. Blue arrows, venules; red arrows, arterioles.



inferonasal sector found in 100% of the animals, the inferotemporal sector (100%), and the superior section (87.5% of the cases). Less frequently, there were venules in the superonasal (12.5%), superotemporal (6.25%), temporal (18.75%), nasal (12.5%), and inferior (12.5%) sectors. The three most frequent sectors (superior, inferonasal, and inferotemporal) reflect the triangular morphology of the venous ring, which was the most frequent.

#### *Retinal arterial circulation in the minipig*

In the optic disk, arterioles emerged more peripherally than veins (central venous ring). Arterioles presented a peculiar layout when emerging from the optic disk. In most cases, their origin was found in the periphery of the optic disk; however, they move centrally when crossing the nerve fiber layer before continuing in a radial pattern toward their corresponding peripheral retinal vascularization areas. Various patterns were presented by arterioles when emerging from the optic disk:

- (1) Peripheral origin, emerging in the periphery of the neuroretinal ring.
- (2) Peripheral origin, emerging in a more central manner in the neuroretinal ring.
- (3) Peripheral origin and running over the surface of the neuroretinal ring, before continuing toward a different section of the optic disk.
- (4) More central origin, found in the center of the optic disk next to the venous ring (Fig. 3).

The first and second arteriolar patterns were most frequently observed, whereas the fourth layout was more frequent in the optic disks containing the hexagonal or quadrangular venous rings.

Retinal arterioles presented medium and small calibers. The total number of retinal arterioles had a mean value of 10.31 (SD = 2), i.e., 5.63 (SD = 1) larger and 4.69 (SD = 2) smaller arterioles.

All arterioles emerged in an independent manner in the different sections of the optic disk, moving with a radial pattern toward the different retinal areas to be irrigated. Arterioles could be observed in all quadrants (superior, temporal, nasal, inferior, superotemporal, inferotemporal, inferonasal, and superonasal). Arterioles appeared more frequently in the nasal and temporal sectors in 81.25% of the animals, followed by fewer arterioles in the superior, inferotemporal, and inferonasal sectors in 68.75% of the animals, and less frequently, in 56.25% of the animals, in the superonasal, and superotemporal quadrants. Lastly, in 50% of the animals arterioles appeared in the inferior sector. Later, along their entire course, they sometimes branched out in a dichotomous and lateral manner providing smaller caliber branches in the retinal equator or periphery.

#### *Arterial/venous crossings*

The choroidal/arterial phase enabled the distinction of the location of arterioles and venules in arteriole-venous crossings. In 70% of the 20 crossings identified in the angiographs, venules were located more internally than arterioles (Fig. 4).

#### *Intraocular pressure*

We found statistically significant differences in IOP between the experimental glaucoma OSs and the control ODs over 14 months of weekly measurements following the first episcleral vein cauterization surgery (week 6). Control ODs had

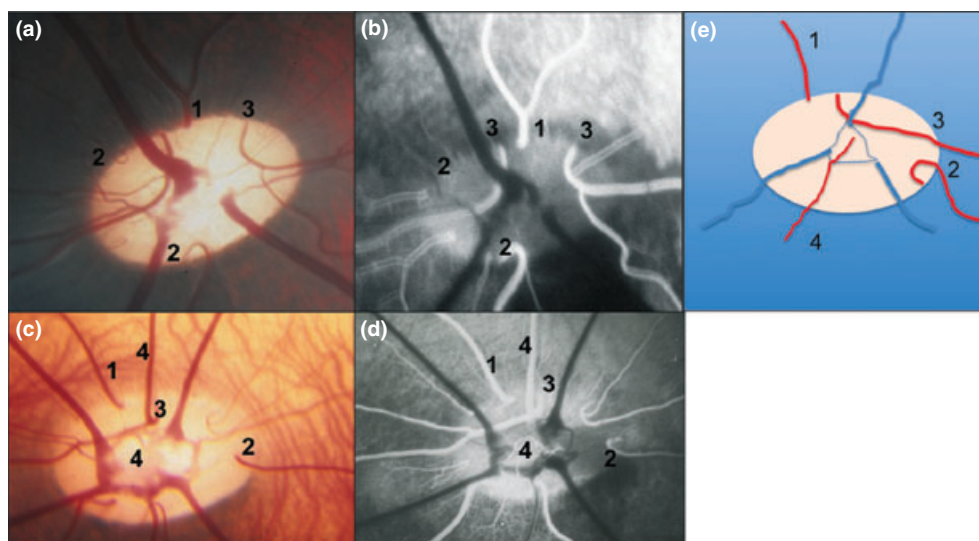


**Figure 3.** Arteriolar types classified according to the pattern with which they emerge from the optic disk. (a–c) Fundus image. (b–d) Fluorescein angiography (choroidal/arterial phase). (e) Schematic: 1. Peripheral origin, emerging in the periphery of the neuroretinal ring. 2. Peripheral origin, emerging in a more central manner in the neuroretinal ring. 3. Peripheral origin and running over the surface of the neuroretinal ring, before continuing toward a different section of the optic disk. 4. More central origin, found in the center of the optic disk next to the venous ring.

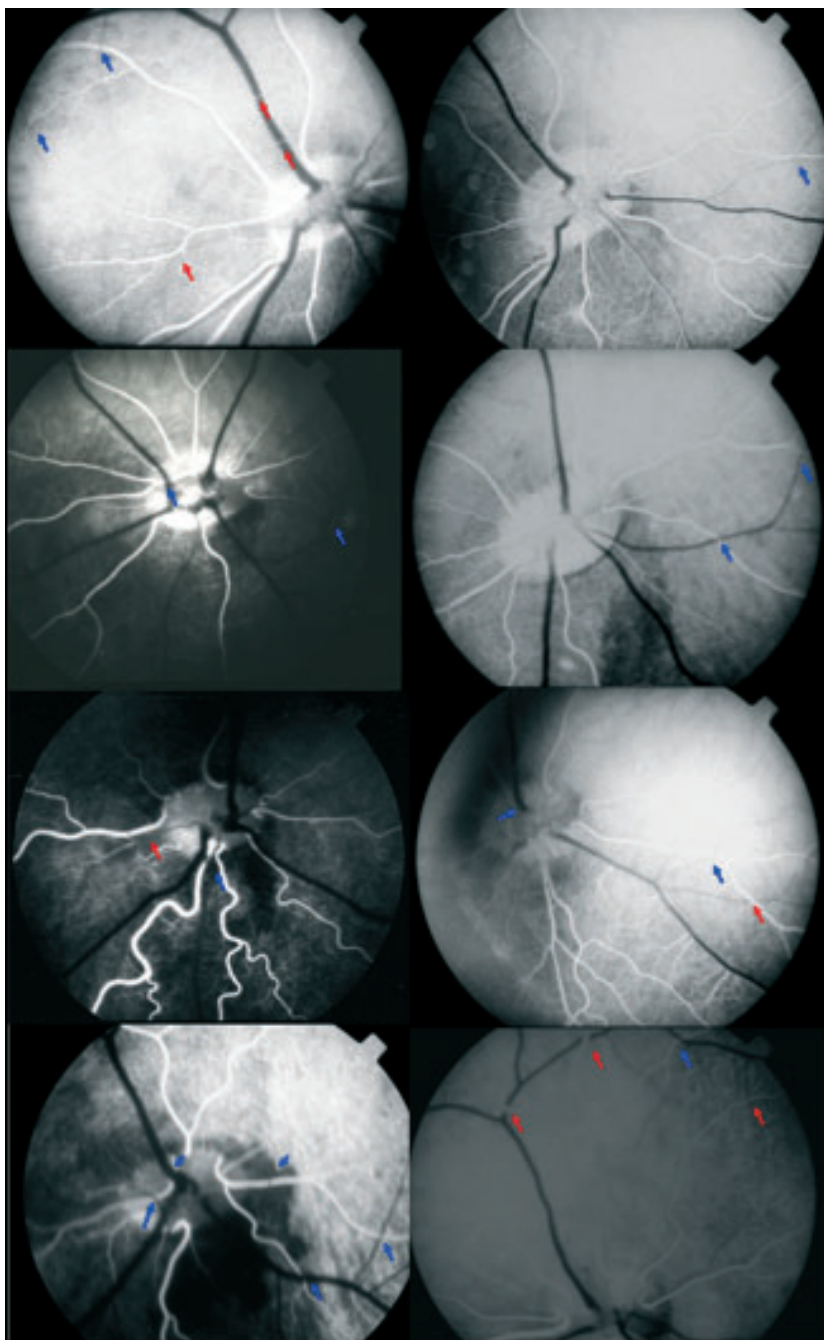


**Figure 4.** Arteriole/venular crossings. Venules are more frequently situated more internally than arterioles in arteriole/venular crossings. The most internal vessel closer to the vitreous cavity is shown for the different crossings. Blue arrows, venules; red arrows, arterioles.

an average IOP of  $22.43 \pm 4.46$  mmHg and glaucomatous OSs  $26.04 \pm 5.01$ , respectively ( $P < 0.01$ ) (Fig. 5).

#### *Fundoscopy changes in glaucoma*

In the minipig experimental glaucoma model, arterioles from a more peripheral origin, emerging centrally in the neuroretinal ring going through the nerve fiber layer (type 2 arterioles), were found to be more incurvated and sometimes incurvated toward the periphery of the neuroretinal ring, when compared to the control eyes (Figs 6 and 7). This arteriole displacement toward the periphery was indicative of the damage of the nerve fiber layer. Of the

animals with experimentally induced glaucoma, 75% showed anatomic differences in the optic disk of their OSs after undergoing surgery to induce a chronic increase in IOP, compared with the baseline level. These changes were observed in 38% of the overall type 2 arterioles in the optic disk. Therefore, these were the primary sentinel vessels that signaled any glaucomatous damage. Once outside of the optic disk, the loss of peripapillary nerve fiber layer may also lead to a medial displacement of the retinal arterioles. In this case, the displacement was independent of the origin of the arteriole in the optic disk. The sentinel vessels that signal the glaucomatous damage in the experimental glau-

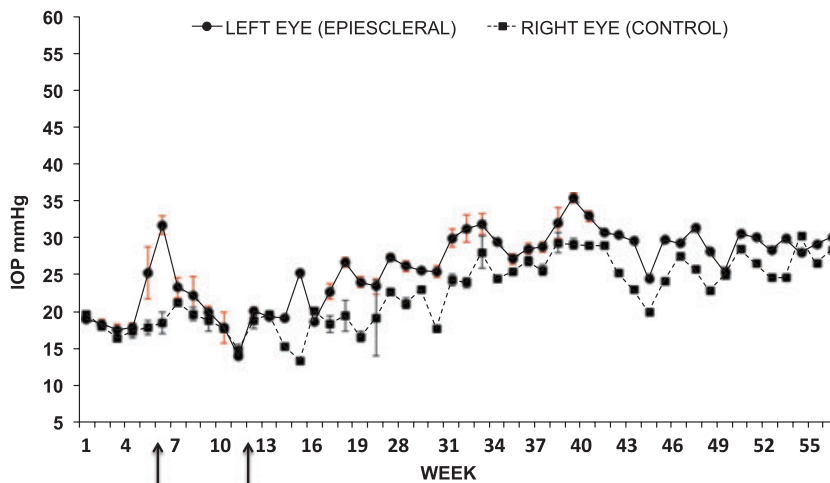


**Figure 5.** Intraocular pressure (IOP) in control and cauterized glaucomatous minipig eyes. Episcleral vein cauterization surgery was carried out firstly in dorsal veins (week six, black arrow) and secondly in ventral veins (week 12, black arrow). From the first surgery in week six, there were significant differences in IOP elevation in OSs, over 52 weeks.

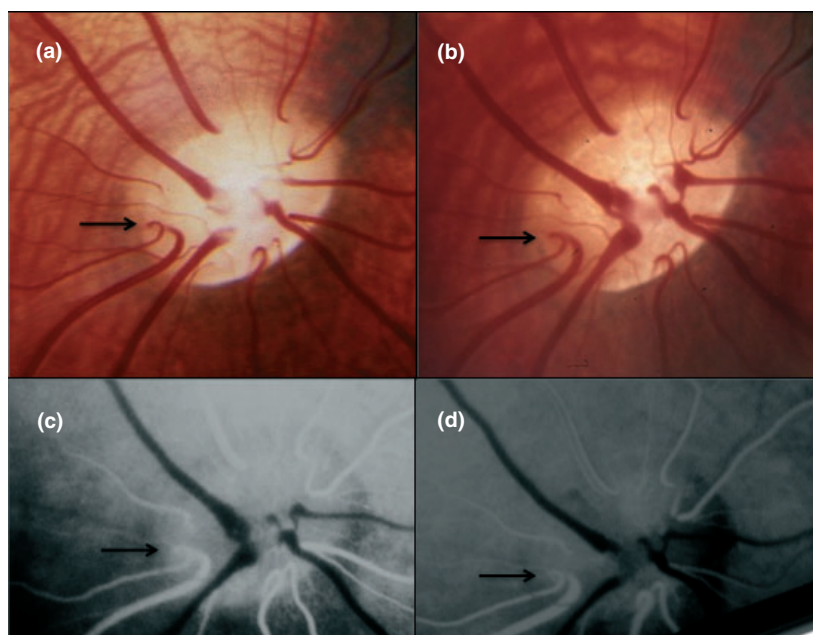


**Figure 6.** Optic disk glaucomatous findings in Göttingen minipig. (a, c) Healthy optic disk of a 5-month-old minipig. (b, d) Optic disk after inducing experimental glaucoma. (a, b) Fundus image; (c, d) Fluorescein angiography (choroidal/arterial phase). A type 2 arteriole is peripherally displaced in the optic disk (black arrow).

coma model in the Göttingen minipig were the retinal arterioles (Fig. 6–7).

#### *Angiographic comparison of the control and glaucoma eye fundus of the Göttingen minipig*

In the comparative study of the control eyes and the eyes undergone episcleral vein cauterization (EVC) with a significant sustained increase in IOP (glaucoma), no significant angiographic differences were observed at the retinal vessel level during equal angiographic phases in both cases. There was a small variation in phase length times (Fig. 8), but these findings were not reproducible.

## DISCUSSION

A description of the morphology of the retinal vessels of the normal and glaucomatous optic disk in the Göttingen

minipig is needed to transfer findings in this experimental model of glaucoma to humans. Although the minipig model presents many similarities to the human eye at the retinal microvasculature level, it is important to detect the differences when interpreting and comparing both species.

The angiographic study of the minipig has previously been analyzed.<sup>10</sup> We would like to highlight the following aspects of the present work when comparing the data presented by Schaepdrijver *et al.*,<sup>10</sup>. The minipigs used were 5 months old, and as previously described, retinal angiography is feasible in young pigs as retinal vasculature is already developed at birth. An ear vein was used instead of the cephalic or saphenous veins. The average limb-fundus time was 3.75 s after intravenous injection into the ear vein, which was less than the cephalic vein injection (9.5 s) and the saphenous vein injection (10.6 s). Regarding the arterial



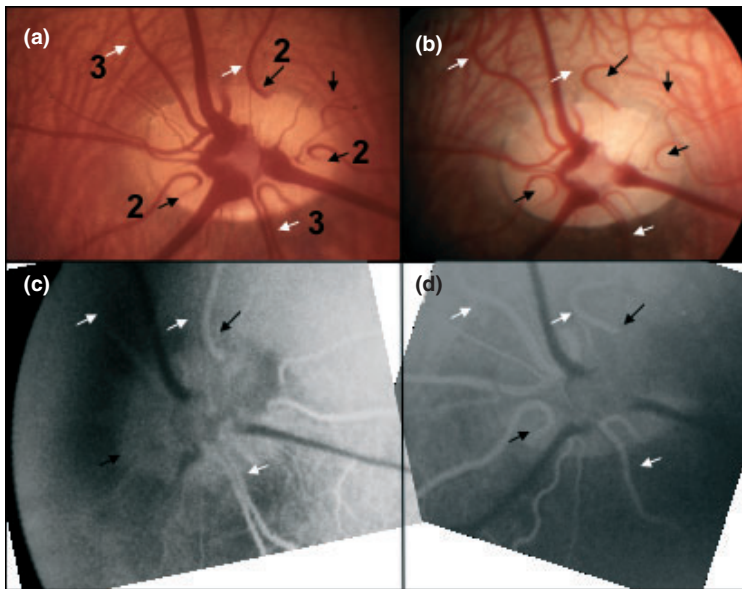


**Figure 7.** Optic disk glaucomatous findings in Göttingen minipigs. (a, c) Healthy optic disk of a 5-month-old minipig. (b, d) Optic disk after inducing experimental glaucoma. (a, b) Fundus image; (c, d) Fluorescein angiography (choroidal/arterial phase). Glaucomatous changes: type 2 arterioles are more incurvated inside the optic disk (black arrows); type 2 and 3 arterioles are medially displaced outside the optic disk (white arrows).

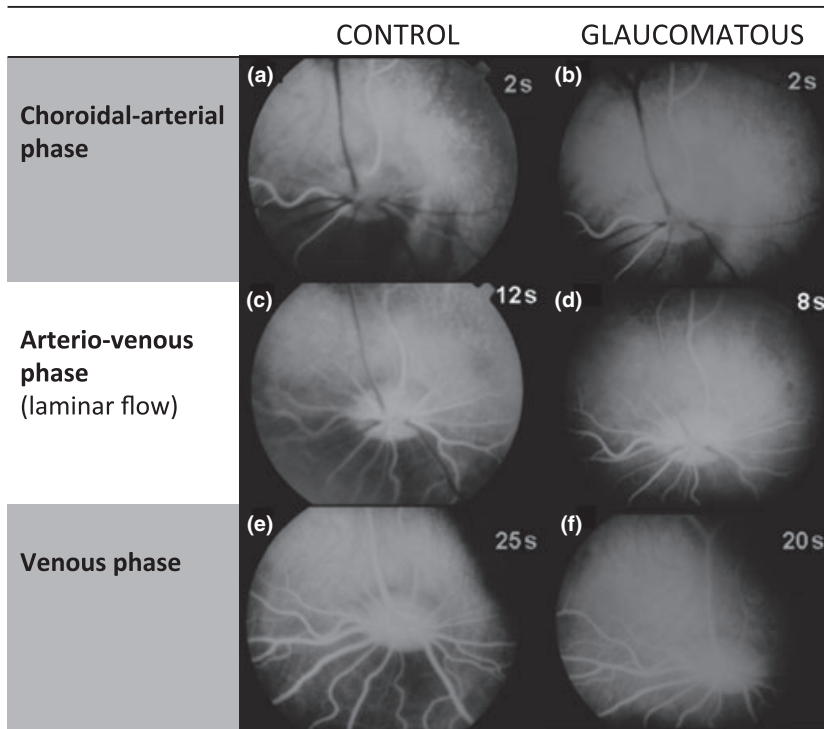


**Figure 8.** Fluorescein angiography in a healthy 5-month-old minipig and after inducing experimental glaucoma over 14 months in the same eye (OS). The different angiography phases are shown: choroidal/arterial phase (a, b), arterial/venous phase (c, d), and venous phase (e, f). The time after the fluorescein injection measured in seconds is indicated in each picture. No significant angiographic differences were observed between control and glaucomatous angiograms in the different phases.

phases already described and matching with the human angiographic pattern, we must point out that we were not able to visualize the isolated choroidal phase in our animals, as it overlapped with the arterial phase, showing a physiological delay of the peridiskal filling until the arterial/venous and venous phases. This peridiskal choroidal delay has already been described in minipigs<sup>10</sup> and it also occurs in humans who show a superior temporal to papilla delay.<sup>29</sup> The optic disk began to show hyperfluorescence during the arterial phase, mostly in the inferior and nasal sectors; later, in the arterial/venous phase, disk fluorescence was complete.

Regarding the study of retinal vascularization in the minipig, various differences with humans have been described. The major differences concern the main orbital vessels of the retinal vascular system. The human eye contains one central retinal artery and one vein that follow a long course next to the optic nerve before reaching the optic disk.<sup>13,17</sup> In the pig, however, retinal blood have not very clear origin<sup>30</sup> but a main artery and one vein also follow the optic nerve before reaching the optic disk.<sup>30</sup> Still, angiographic and vascular corrosion studies demonstrate that larger retinal venules are more central in the optic disk than



arterioles and that they normally converge in a venous circle in the optic disk.<sup>10</sup>

In our study, we analyzed the location of the arterioles and venules when emerging from the optic disk, together with their distribution by optic disk sector when moving toward retinal areas to vascularize the control and glaucomatous eyes, to compare them with findings from the human model.

We found slight differences when comparing human and minipig retinal vascularization emerging from the optic disk. In the human, the arterial and venous system is highly symmetric (regarding the origin and course of the vessels, which are practically parallel); however, in the minipig, there are two asymmetric systems in most cases. Minipig arterioles are found in greater numbers, and they emerge from almost all optic disk sectors in a more peripheral manner, while there are less main venules and they converge in a common venous ring in the center of the optic disk. This occurs in the most common morphology pattern of the venous ring, the triangular pattern, as well as in others such as the quadrangular patterns. We only found a vascularization model in one minipig which presented a venous system with a hexagonal ring, where the arterial and venous systems were more symmetric regarding the number of vessels, origin, and course. In no case was a complete arteriolar ring observed, but various arterioles were observed in some animals in the center near the venous ring, probably branching from a common central arterial stem.

In our work, the retinal arterial circulation in the minipig had an average number of 10 arterioles, with an average of six with a larger caliber and an average of five with a smaller caliber, corresponding well with the data previously reported of three or four main retinal arterioles with a luminal diameter of 100  $\mu\text{m}$ , and 2–5 small arterioles with a lumen of 50  $\mu\text{m}$ .<sup>11</sup> The main venules presented an average number of 7. Two well-differentiated calibers of venules converged in the central venous ring; the greater caliber venules presented an average number of four and the smaller caliber venules also presented an average of 4, data similar to that of Simoens *et al.*<sup>11</sup> who reported the existence of three or four main retinal venules with a lumen diameter of 100–200  $\mu\text{m}$  and around five venules with a diameter smaller than 100  $\mu\text{m}$ .<sup>11</sup> The morphology of the venous ring in the animals studied was primarily determined by large caliber venules. We observed at least four different venous ring morphologies: triangular (three main venules), rhomboidal and quadrangular (four main venules), and hexagonal (6–7 main venules). The sectors covered by the arterial and venous systems were also different both in number of sectors, as well as in location. Arterioles emerge in an independent manner in the optic disk, and move in a radial pattern toward the retinal regions to be vascularized, occupying different optic disk sectors. The venous system, less numerous, occupies fewer sections when crossing through the neuroretinal ring of the optic disk. There are three principal sectors where the larger-sized venules join together toward

the venous ring, reflecting the most frequent triangular morphology of the venous ring: the inferonasal sector, found in all the animals, the inferotemporal sector (also in 100%), and lastly, the superior sector found in 87.5% of the cases. Regarding the arteriole-venular crossings, while in the human eye retinal arterioles are mostly found more internally than venules,<sup>13,17</sup> the minipig venules are found more internally than arterioles in 70–80% of the cases,<sup>10,11</sup> contrary to the affirmations of other authors that retinal arterioles in the pig are found more internally than the venules.<sup>31,32</sup>

Regarding the retinal circulation, in all of the eyes studied, arterioles mostly emerged from the periphery of the optic disk, and although they occasionally moved directly to the vascularization of a retinal area (type 1 pattern), type 2 pattern arterioles, emerging in a more central manner in the neuroretinal ring, were more frequent. Occasionally, arterioles were found on the surface of the neuroretinal ring, which then emerged from another disk sector (type 3 pattern), or less frequently, several arterioles emerged from a common central arterial stem (type 4 pattern). Type 2 arteriole patterns were modified in the experimental glaucoma, with a greater displacement and peripheral incurving, indicating the loss of nerve fiber layer of the neuroretinal ring.

A normal papilla in humans shows a pattern that has a consistent rim width following the ISNT rule.<sup>24</sup> However, it is very difficult to accurately delimit the area of the neuroretinal ring in the minipig optic disk. The fact that the multi-vascular central venous ring occupies the entire center of the optic disk corresponding with the lamina cribosa makes it impossible to differentiate the salmon color of the neuroretinal ring that contrasts with the pale color of the lamina cribosa, as occurs in humans.

Although certain findings associated with glaucoma in humans, such as the exposure of the lamina cribosa and the discovery of circumlinear vessels,<sup>28</sup> might also appear in the glaucomatous minipig, they were more difficult to detect. Peripheral nasal rejection of retinal vessels (arterioles and venules), which is typical in humans,<sup>28</sup> corresponded with an incurvation and sometimes peripheral rejection in the optic disk of type 2 arterioles in minipigs (Fig. 6), indicating the glaucomatous lesion of the optic disk. The possibility of finding a medial displacement of the vessels was present in minipigs, but with some differences to that found in humans. There was an important medial displacement in type 2 and 3 arterioles, once outside of the optic disk, corresponding with the loss of the layer of peripapillary nerve fibers (Fig. 7). These findings could be explained by the very superficial location of the porcine retinal vessels in the nerve fiber layer and with a protruding position,<sup>11,33</sup> when compared with humans. This might make them more sensitive to the displacement from the loss of the layer of retinal fibers. In humans with primary open-angle glaucoma (POAG), there are nonspecific changes inside the optic disk such as a nasal peripheral displacement of all vessels (arterioles and venules), thus showing an excavation (loss of neuroretinal ring)

and the clear exposure of the lamina cribosa.<sup>26,28</sup> Angiographic changes have been described in the porcine models of acute glaucoma, showing a slowing in the flow velocity in retinal vessels and in the choroidal/arteriolar retinal filling.<sup>34</sup> However, in our model of chronic open-angle glaucoma with EVC, we found no angiographic differences in the eyes with experimental glaucoma compared with the control eyes, as occurred in the human eyes. Therefore, neither surgery with EVC nor IOP-induced changes in the chorioretinal circulation.

To conclude, the differences of the minipig arteriolar and venular vasculature emerging from the optic disk compared with that of humans include, first of all, a greater asymmetry of the arteriolar and venular system in the minipig, and a different pattern of the arteriolar system when emerging from the optic disk. The arterioles are more numerous, present a smaller diameter, and occupy more sectors, the most frequent being the temporal and nasal sectors, followed by the superior, inferotemporal, and inferonasal sectors. Arterioles emerge from the periphery of the optic disk usually moving centrally to emerge between the nerve fiber layer of the optic disk neuroretinal ring (type 2 arterioles).

In the experimental glaucoma model, the displacement of the vessels in the optic disk was observed in the neuroretinal ring just as occurs in humans with POAG. In minipigs with experimental glaucoma, some arterioles (type 2 and 3) were nasally displaced and incurved medially once outside of the optic disk, contrary to the nasal peripheral displacement of all retinal vessels (arterioles and venules) inside the optic disk in humans. In minipigs, the central venous ring is formed by various vessels and occupies the center of the optic disk, making visualization of the lamina cribosa difficult. In addition, the minipig venous ring does not suffer evident modifications as a result of experimental glaucoma.

These findings allow the identification of glaucomatous changes in the experimental glaucoma model in minipigs, and their comparison with those of human POAG, which is important to transfer data from the animal model to the human.

#### ACKNOWLEDGMENTS

Spanish Ministry of Science and Technology (SAF 2007-62060), Ayudas Grupos Consolidados Gobierno Vasco (IT437-10), ONCE Foundation (Spain), BIOEF08/ER/006, Fundación Jesús Gangoiti Barrera, Red Patología Ocular RETICS (RD07/0062).

#### REFERENCES

- Galdos M, Bayón del Río A, Micó Valls C *et al.* Funduscopy and ultrastructural evaluation in experimental glaucoma model in minipigs (abstract). *ARVO Annual Meeting 2010*. Abstract 6392.
- Ruiz-Ederra J, García M, Hernández M *et al.* The pig eye as a novel model of glaucoma. *Experimental Eye Research* 2005; **81**: 561–569.
- Ruiz-Ederra J, García M, Martín F *et al.* Comparison of three methods of inducing chronic elevation of intraocular pressure in the pig (experimental glaucoma). *Archivos de la Sociedad Española de Oftalmología* 2005; **80**: 571–579.
- García M, Ruiz-Ederra J, Hernández-Barbáchano H *et al.* Topography of pig retinal ganglion cells. *The Journal of Comparative Neurology* 2005; **486**: 361–372.
- Suarez T, Vecino E. Expression of endothelial leukocyte adhesion molecule 1 in the aqueous outflow pathway of porcine eyes with induced glaucoma. *Molecular Vision* 2006; **12**: 1467–1472.
- Balaratnasingam C, Morgan WH, Bass L *et al.* Time-dependent effects of elevated intraocular pressure on optic nerve head axonal transport and cytoskeleton proteins. *Investigative Ophthalmology and Visual Science* 2008; **49**: 986–999.
- García M, Forster V, Hicks D *et al.* Effects of Müller glia on cell survival and neurogenesis in adult porcine retina in vitro. *Investigative Ophthalmology and Visual Science* 2002; **43**: 3735–3743.
- García M, Forster V, Hicks D *et al.* In vivo expression of neurotrophins and neurotrophin receptors is conserved in adult porcine retina in vitro. *Investigative Ophthalmology and Visual Science* 2003; **44**: 4532–4541.
- Lind NM, Moustgaard A, Jelsing J *et al.* The use of pigs in neuroscience: modeling brain disorders. *Neuroscience and Biobehavioral Reviews* 2007; **31**: 728–751.
- De Schaepdrijver L, Simoons P, Pollet L *et al.* Morphologic and clinical study of the retinal circulation in the miniature pig. B: Fluorescein angiography of the retina. *Experimental Eye Research* 1992; **54**: 975–985.
- Simoens P, De Schaepdrijver L, Lauwers H. Morphologic and clinical study of the retinal circulation in the miniature pig. A: Morphology of the retinal microvasculature. *Experimental Eye Research* 1992; **54**: 965–973.
- Bloodworth JM, Gutgesell HP, Engerman RI. Retinal vasculature of the pig. Light and electron microscopic studies. *Experimental Eye Research* 1965; **4**: 174–178.
- Hogan MJ, Alvarado JA, Weddel JE (eds). *Histology of the Human Eye. An Atlas and Textbook*. WB Saunders, Philadelphia, 1971.
- Shimizu K, Ujiie K. *Structure of Ocular Vessels*. Igaku-Shoin, Tokyo, 1978.
- Ernest JT, Stern WH, Archer DB. Submacular choroidal circulation. *American Journal of Ophthalmology* 1976; **81**: 574–582.
- Ujiie K. Three-dimensional view of the retinal capillary. *Nippon Ganka Gakkai Zasshi* 1976; **80**: 634–644.
- Fine BS, Yanoff M. *Ocular Histology. A Text and Atlas*, 2nd edn. Harper & Row, New York, 1979.
- Duke-Elder S, Wybar SC. *The Anatomy of the Visual System. System of Ophthalmology*, Vol. II. H. Kimpton, London, 1961:339–382.
- Araki M. Observations on the corrosion casts of the radial peripapillary capillaries. *Acta Societatis Ophthalmologicae Japonicae* 1976; **81**: 982–993.
- Prince JH, Diesem CD, Eglitis I *et al.* Anatomy and histology the eye and orbit in domestic animals. In: *The Pig* (ed Thomas CC). Charles C Thomas, Springfield, 1960; 210–230.
- Rootman J. Vascular system of the optic nerve head and retina in the pig. *British Journal of Ophthalmology* 1971; **55**: 808–819.
- Hayreh SS. Recent advances in fluorescein fundus angiography. *The British Journal of Ophthalmology* 1974; **58**: 391–412.
- De Lacy JJ. Fluorescein angiography of the choroid in health and disease. *International Ophthalmology* 1983; **6**: 125–138.
- Jonas JB, Gusek GC, Naumannn GOH. Optic disc cup and neuroretinal rim size, configuration and correlations in normal eyes. *Investigative Ophthalmology and Visual Science* 1988; **29**: 1151–1158.

25. Tuulonen A, Airaksinen PJ. Initial glaucomatous optic disk and retinal nerve fiber layer abnormalities and their progression. *American Journal of Ophthalmology* 1991; **111**: 485–490.
26. Nicolela MT, Drance SM, Broadway DC *et al.* Agreement among clinicians in the recognition of patterns of optic disk damage in glaucoma. *American Journal of Ophthalmology* 2001; **132**: 836–844.
27. European Glaucoma Society. *Terminology and Guidelines for Glaucoma*, 2nd edn (ed. Dogma). Savona, Italy, 2008.
28. Cantor L, Fechtner RD, Michael AJ *et al.* *Basic and Clinical Science Course Section 10: Glaucoma*. American Academy of Ophthalmology, San Francisco, 2001.
29. Richard G, Soubrane G, Yanuzzi L. *Fluorescein and ICG Angiography. Textbook and Atlas*, 2nd edn. Thieme, Germany, 1998.
30. Simoens P. Morphologic study of the vasculature in the orbit and eyeball of the pig. Thesis, University of Ghent, 1985.
31. Michaelson IC, Friedenwald JS. *Retinal Circulation in Man and Animals*. Charles C. Thomas, Springfield, 1954.
32. Wise GN, Dollery CT, Henkind P. *The Retinal Circulation*. Harper & Row, New York, 1971.
33. Ashton N, Dollery CT, Henkind P *et al.* Focal retinal ischaemia. Ophthalmoscopic, circulatory and ultrastructural changes. *The British Journal of Ophthalmology* 1966; **50**: 281–324.
34. Dollery CT, Henkind P, Kohner EM *et al.* Effect of raised intraocular pressure on the retinal and choroidal circulation. *Investigative Ophthalmology* 1968; **7**: 191–198.